LiV_3O_8 Nanoplates Via Polyacrylamide-assisted Freeze Drying Method and as Cathode Materials for Li-ion Batteries

Lin Li[1, 2,*], *Wei* Zheng[1], *Rongfei* Zhao[1] and *Jinsong* Cheng[1]

[1]School of Chemistry and Chemical Engineering ,Anshun University, Anshun 561000, China
[2]School of Chemical Engineering, Guizhou University of Engineering Science, Bijie 551700, China

Abstract. The LiV_3O_8 nanoplates cathode materials was prepared by polyacrylamide-assisted freeze drying method. The annealing temperature affected the agrochemical properties of the LiV_3O_8 nanosheets cathode materials. The LiV_3O_8 nanoplates cathode materials were characterized by XRD, XPS, SEM, TEM, and galvanization charge/discharge profile measurement. The LiV_3O_8 fabricated at 550 ^oC (LVO550) showed the highest discharge capacity, best agrochemical performance, and high rate capability (after 100th, a reversible discharge capacity up to 223.8 mAh g^{-1}). Benefiting from two dimensional nanoplates structure can provided a larger surface area, shorter lithium ion diffusion path, and maintain stable structure, the LiV_3O_8 nanoplates exhibited excellent rate capability, high reversible capacity and high temperature properties.

1 Introduction

Lithium ion battery (LIBs) have been more and more widely used with pure electric vehicles, hybrid electric vehicles, mobile electronic products, et.al [1]. However, commercialization cathode material of the $LiCoO_2$ (expensive of the raw material and environmental pollution problems of Co element) and $LiFePO_4$ (low electrical conductivity) limit the further development and application of LIBs [2]. So the development of low cost, non-toxic, long cycle life of electrode materials become the urgent demand of the LIBs [3]. The LiV_3O_8 layered compounds as a cathode materials, have attracted much attentions, due to good safety, low cost, their high theoretical capacity (~ 280 mAh g^{-1}), and easy preparation [4]. But, the LiV_3O_8 show poor cycle performance in the process of charging and discharging, thus restricting its development and large-scale application, and need further improvement [5]. Several approaches of doping modification, surface coating, and synthesis of specific nanostructures have been deployed to achieve those issues [6]. In these modification methods, synthesis of specific nanostructures can effectively improved the cycle performance, because of the specific nanostructures electrodes provided large contact area with the electrode material/electrolyte and short ions diffusion path [7].

A lot of research results show that the morphology, particle size and crystallinity of electrode materials have a very important influence to cycle performance and rate

* Corresponding author: 404003375@qq.com

performance[8]. The 2D nanoplates can effectively offered larger specific surface area and short electronic transmission path. This is mainly due to nano effect of the one dimensional structure can improved the electrochemical performance, and the axial microstructures can guaranteed the thermodynamic stability [9]. However, because of the LiV_3O_8 layered structure, the two dimensional structure of electrode materials were difficultly synthesized. Feng et.al [5] prepared the LiV_3O_8 via a sol-gel and solid-state method, the LiV_3O_8 materials display a high reversible capacity. Herein, the LiV_3O_8 nanosheets were prepared via a polyacrylamide-assisted freeze drying method. The electrochemical performances, structure, and morphology for the LiV_3O_8 nanoplates have been studied. Compared with the traditional preparation method, the LiV_3O_8 nanoplates exhibited excellent capacity and high temperature properties.

2 Experimental

0.03 mol of V_2O_5 and 0.01 mol of $LiOH{\cdot}H_2O$ were added into 80 mL of de-ionized water and stirring, and 0.18 mol of $C_2H_2O_4{\cdot}H_2O$ was added into the mixed solution was vigorously stirred for 2 h, then 2 g polyacrylamide was added into the mixed solution was vigorously stirred for 1.5 h. Afterwards, the process of freeze drying could be briefly shown in ref [10]. The sticky precursors were calcined at 450, 500, 550, and 600 °C for 4 h to obtain the LiV_3O_8 samples. The as-synthesized oxides were designated as LVO450, LVO500, LVO550, and LVO600.

An SEM (JEOLJSM-7400F, Japan), TEM (JEM-2010, Japan), XPS, and X-ray diffractometer (XRD, D8 Advance, Bruker AXS) were used to detect structure and morphology of the LiV_3O_8 samples. The typical Electrochemical measurements process of LiV_3O_8 material could be briefly shown in ref [10].

3 Result and discussion

Figure.1 showed the XRD patterns of the those LiV_3O_8 samples. The diffraction peaks can be indexed to LiV_3O_8 (JCPDS No.72-1193). And the identified diffraction peaks at 50.8°, 42.1°, 40.9°, 40.3°, 30.7°, 28.5°, 26.1°, 23.3°, 15.6°, and 13.8°can be well assigned to (020), (203), (-205), (-301), (103), (-111) , (-202), (003), (002), and (100) planes of the layer structure LiV_3O_8. These samples exhibit sharp diffraction peaks, indicating the well crystallization. XPS experiments were performed to identify the chemical composition and the oxidation states of the LVO550 sample in Fig. 1c. The complete XPS spectra indicate the existence of Li, O, and V elements. The two peak at 516.9 and 524.4 eV corresponds to V 2p3/2 and V 2p1/2, respectively. The O 1s peak at 529.7 eV for V-O and Li-O bonds.

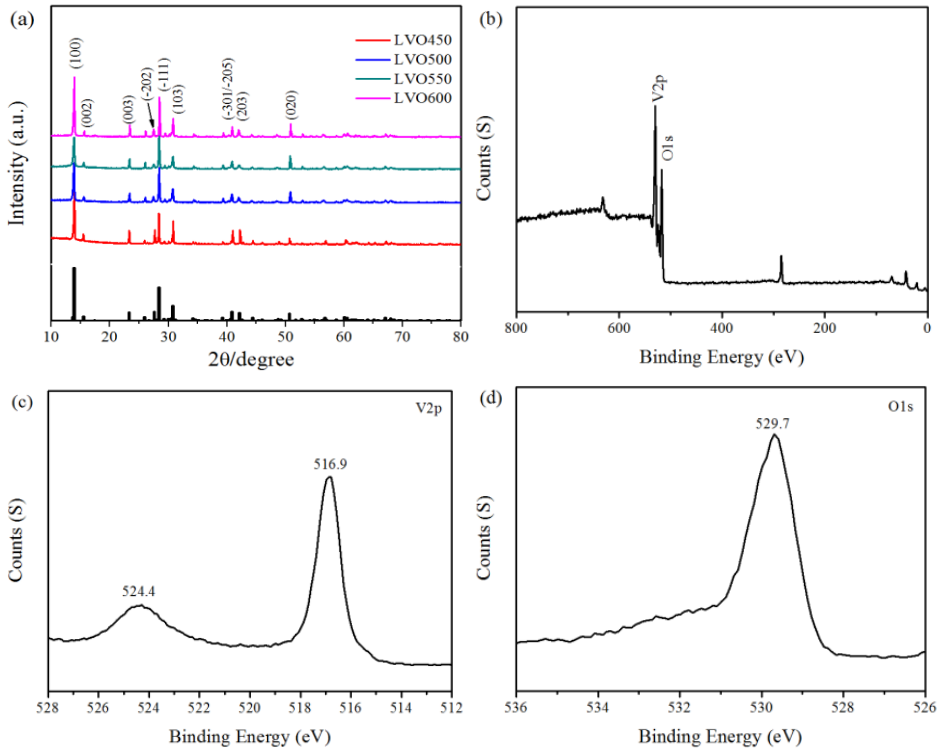

Fig. 1. XRD patterns of all LiV_3O_8 samples, (b) XPS survey spectrum of LVO500 and high-resolution XPS spectra of (c) V 2p and (d) O1s.

The LVO450, LVO500, LVO550, and LVO650 samples were measured via scanning electron microscopy (SEM). The non-uniform size of LVO450 samples can be founded in Fig. 2a, low-magnification SEM show the β-MnO_2 sample is composed of nanoplates (a small amount) and non-uniform nanorods. After high temperature calcination of 550 and 600 ^oC, compared with the LVO450 sample, those samples maintained the nanoplates morphology (diameters of 0.5-1.0 μm, length of 0.5-2.0 μm), the diameter is increased and the length is shorted. This may be due to the nanorods produced swelling effect along the axis direction with the embedding of Li^+ in high temperature heat treatment process. As observed in the HRTEM image (in Fig2. f), the expanded dspacing (~ 0.22 nm) of (−301/−205) planes of LiV_3O_8 [9]. In addition, Fig. 2e show a nanoplates morphology of diameters of 500-1000 nm of the LVO550 sample.

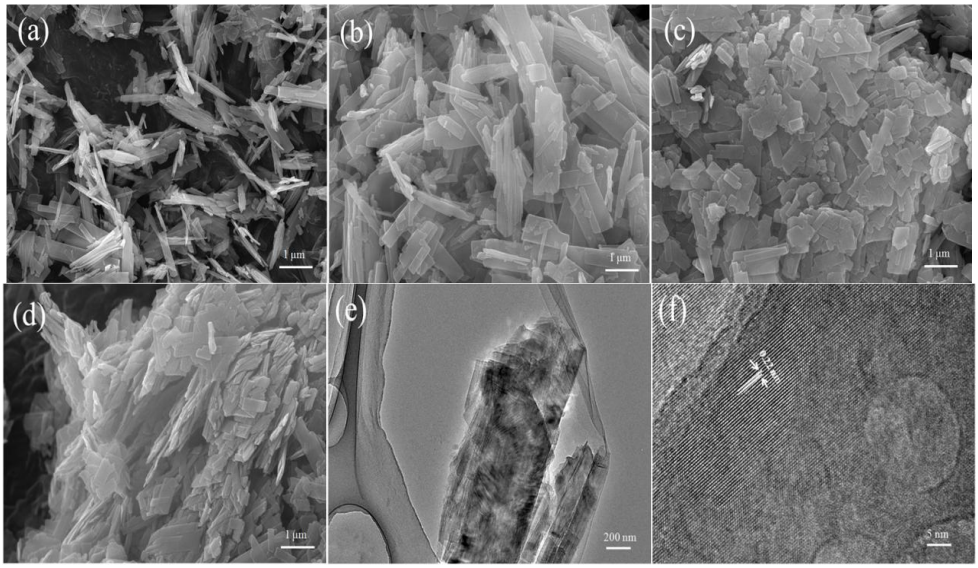

Fig.2. SEM images of (a) LVO450, (b) LVO500, (c) LVO550, and (d) LVO600, Fig. 4 (a) TEM/HRTEM image (e, f) of LVO550.

To investigate the half-cell performances of the LiV_3O_8 samples, GCD (galvanostatic charge-discharge) and CV (cyclic voltammograms) were carried out at 100 mAh g^{-1} of 2.0–4.0 V. The first discharge capacity of the LVO600, LVO550, LVO500, and LVO450 were 240, 267, 220, and 292 mAh g^{-1}, and the capacity of 170, 224, 187, and 112 mAh g^{-1} after 100 cycle, retention were 70.1, 83.8, 85.0, and 41.7 % from the first cycle, respectively. The rate capability of the LVO600, LVO550, LVO500, and LVO450 electrode is illustrated in Fig. 3e. Compared with other electrodes, the LVO550 electrode showed specific capacities of 303.7 223.7, 198.2, 187.9, 169.8, 137.2, 117.6 mAh g^{-1} at 100, 300, 600, 1500, 3000, 6000, and 10000 mA g^{-1}, respectively. The LVO550 electrode exhibits higher capacity compare to other electrode indicating faster diffusion of lithium-ion. Outstanding electrochemical properties for the LiV_3O_8 nanoplates attributed to two dimensional nanoplates structure can provided a larger surface area, shorter lithium ion diffusion path, maintain stable structure, guaranteed the good rate performance [11]. Fig. 3g shows cyclic voltammograms of LVO550 sample. The first cathodic peak appeared at ~ 2.46 V, 2.70 V, 2.76 V, 2.96 V, and 3.63 V, which related to the insertion of Li-ion into the LiV_3O_8 materials and transform to $Li_{1+x}V_3O_8$ (x = 0.1–3) couples in the reduction process. And the broad peak appears at ~ 2.42 V, 2.82 V, 2.88 V, and ~ 3.70 V, which is due to the conversion of impurity V_2O_5 and $Li_{0.3}V_2O_5$ active phase formation in the oxidation process. In subsequent cycles, no changes of the potentials observed, suggesting the good stability of the LVO550 material. Fig. 3h shows EIS test of the LiV_3O_8 samples. The result of charge transfer resistance and solid phase diffusion were described to the semicircle and straight line of the EIS cycles. The R_{ct} value of the LVO600, LVO550, LVO500, and LVO450 electrodes are 110Ω, 73 Ω, 89 Ω, and 142 Ω, indicating that LVO550 electrode own lithium ion diffusion and rapid charge transfer with the others sample, indicating that the LVO550 electrode own rapid charge transfer and lithium ion diffusion with the others sample. It is demonstrated that an enhanced cycle performance can be acquired because nanoplates structure can accelerate the electron diffusion and effectively accommodate the volume variation during the discharge/charge process and offer short pathways for the ions as well as electrons [12].

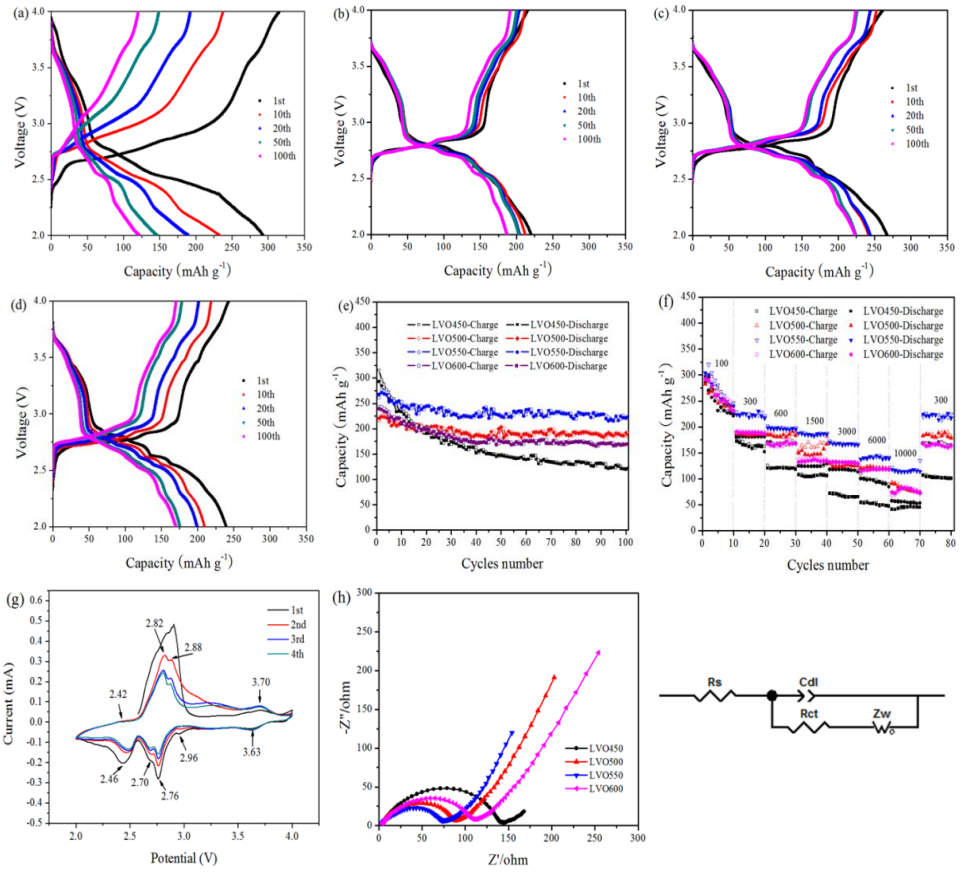

Fig.3. Discharge–charge curves of (a) LVO450, (b) LVO500, (c) LVO550, and (d) LVO600, (e) cycling performance and (f) rate performance of the LVO450, LVO500, LVO550, and LVO600; (g) cyclic voltammograms of LVO550 electrodes; (h) EIS of the LVO450, LVO500, LVO550, and LVO600.

4. Conclusions

In summary, the LiV_3O_8 nanoplates cathode materials was prepared by polyacrylamide-assisted freeze drying method. The annealing temperature affected the agrochemical properties of the LiV_3O_8 nanosheets cathode materials. The LiV_3O_8 nanoplates cathode materials were characterized by XRD, XPS, SEM, TEM, and galvanization charge/discharge profile measurement. The LiV_3O_8 fabricated at 550 ^oC (LVO550) showed the highest discharge capacity, best agrochemical performance, and high rate capability (after 100th, a reversible discharge capacity up to 223.8 mAh g^{-1}). Benefiting from two dimensional nanoplates structure can provided a larger surface area, shorter lithium ion diffusion path, and maintain stable structure, the LiV_3O_8 nanoplates exhibited excellent rate capability, high reversible capacity and high temperature properties.

Acknowledgments

Financial support provided by the Guizhou Provincial Education Department (KY [2018] 031).

References

[1] W.S. Chen, H.P. Yu, S.Y. Lee, T. Wei, J. Li, Z.J. Fan, Chem. Soc. Rev. **47**, 2837 (2018)

[2] X. Guo, G. Zhang, Q. Li, H. Xue, H. Pang, Energy Storage Mater. **15**, 171 (2018)

[3] B. Dunn, H. Kamath, J.M. Tarascon, Science **334**, 928 (2011)

[4] H. Zheng, Q. Zhang, H. Gao, W. Sun, H.M. Zhao, C.Q. Feng, J.F. Mao, Z.P. Guo, Energy Storage Mater. **22**, 128 (2019)

[5] L.L. Feng, W. Zhang, L.N. Xu, D.Z. Li, Y.Y. Zhang, Solid State Sciences **103**, 106187 (2020)

[6] H. Baea, Y. Kim, Mater. Adv. **2**, 3234 (2021)

[7] J.H. Stansby, N. Sharma, D. Goonetilleke, J. Mater. Chem. A **8**, 24833 (2020)

[8] M.S. Ziegler, J.E. Trancik, Energy Environ. Sci. **14**, 1635 (2021)

[9] Z. Chen, F. Xu, S. Cao, Z. Li, H. Yang, X. Ai, Y. Cao, Small **13**, 18 (2017)

[10] L.P. Wang, L.B. Deng, Y.L. Li, X.Z. Ren, H.W. Mi, L.N. Sun, P.X. Zhang, Y. Gao, Electrochimica Acta **284**, 366 (2018)

[11] L.L. Feng, W. Zhang, L.N. Xu, D.Z. Li, Y.Y. Zhang, J. Alloy. Compd. **103**, 106187 (2020)

[12] S. Huang, X.L. Wang, Y. Lu, X.M. Jian, X.Y. Zhao, H. Tang, J.B. Cai, C.D. Gu, J.P. Tu, J. Alloy. Compd. **584**, 41 (2014)